Supporting Information

Establishing a new hot electrons transfer channel by ion doping in plasmonic metal/semiconductor photocatalyst

Zhiyu Wang,[a] Jiawei Xue,[b] Haibin Pan,[a] Lihui Wu,[a] Jingjing Dong,[a] Heng Cao,[a] Song Sun,[a,c] Chen Gao,[a,d] Xiaodi Zhu*[a] and Jun Bao*[a]

[a] National Synchrotron Radiation Laboratory, University of Science and Technology of China, Hefei, Anhui, 230029, China.

[b] The Institute of Scientific and Industrial Research, Osaka University, Mihogaoka 8-1, Ibaraki, Osaka 567-0047, Japan

[c] School of Chemistry and Chemical Engineering, Anhui University, Hefei, Anhui, 230601, China.

[d] Beijing Advanced Sciences and Innovation Center of Chinese Academy of Sciences, Huairou, Beijing, 101407, China.

*Corresponding author.

* E-mail: zhuxiaodi@ustc.edu.cn; baoj@ustc.edu.cn

Experimental details

Samples synthesis

The pure TiO_2 and Fe-TiO_2 nanoplates were prepared by the hydrothermal method using tetra-n-butyl titanium ($Ti(OC_4H_9)_4$) as the precursor.[1] The detailed procedure was as follows: 9 mL HF (as shape-directing agent) solution was added drop-wise into 30ml $Ti(OC_4H_9)_4$ and the obtained solution was stirred for 30 min. Then the obtained solution was put into Teflon autoclave and heated at 204 ^oC for 48 h to acquire TiO_2 nanoplates with highly exposed (001) facets. After cooling down to room temperature, the precipitate was washed by distilled water and ethanol for 10 times to remove the excess HF and dried at 60 ^oC for 10 h to obtain the pure TiO_2 powder. For the Fe-TiO_2 photocatalyst, the Fe dopant was introduced by adding a certain amount of $Fe(NO_3)_3$ aqueous solution (according to the initial feed ratio of Fe/Ti: = 0.7 wt%) in Teflon autoclave and heated at 204 ^oC for 10 hours.[2]

Ag nanoparticles were loaded on TiO_2 and Fe-TiO_2 surface by using a typical photocomposition method.[3, 4] An aqueous suspension of 0.1 g TiO_2 or Fe-TiO_2 powder with 20 ml 1 M methanol (as an electron donor) and 2 ml $AgNO_3$ (1wt%) solution was stirred and sonicated in 78 mL pure water. After irradiation with 300 W xenon lamp for 10 min, Ag/TiO_2, Ag/Fe-TiO_2, were produced.

Characterization

X-ray diffraction (XRD) pattern was carried out on a Rigaku X-ray Diffractometer (TTR-III) with Cu-Kα radiation at a scan rate of 10°C/min. X-ray photoelectron spectroscopy (XPS) and the corresponding valence band spectra was measured on the Thermo ESCALAB 250 XPS system with a monochromatized Al Kα X-ray source (1486.6 eV). All binding energies were corrected for charge shift by subtracting the C 1s peak of surface adventitious carbon at 284.8 eV. Transmission electron microscopy (TEM) was performed on the JEM-2010 transmission electron microscope and high-resolution image was recorded on the JEM-2100F field emission transmission electron microscope. UV-visible diffuse reflectance spectra (UV-vis DRS) was recorded by the UV-visible absorption spectrometer (UV-2700, SHIMADZU) in the wavelength range of 300-650 nm, using $BaSO_4$ as the reference. The actual amount of Fe dopant was determined by inductively coupled plasma atomic emission spectrometry (ICP-AES) (Optima 7300 DV).

The synchrotron radiation X-ray Absorption Near Edge Structure (XANES) experiments were conducted measured at the photoemission end-station at beamline BL10B in the National Synchrotron Radiation Laboratory (NSRL) in Hefei, China. A bending magnet is connected to the beamline, which is equipped with three gratings covering photon energies from 100 to 1000 eV. In this experiment, the XANES was measured in the

total electron yield (TEY) mode under an ultrahigh vacuum at 5×10^{-10} mbar. The resolving power of the grating is typically $E/\triangle E = 1000$, and the photon flux was 1×10^{10} photons/s. All the as-prepared samples are evenly spread on separated conductive tapes and transferred to vacuum chamber. The 300 W xenon lamp (CEL-HXF300E, CEAULIGHT Co., Ltd.) was used as the light source during the XANES measurements. All the spectra at both Fe L-edge and Ti L-edge were collected in 0.2 eV energy steps. The XANES raw data were normalized by a procedure consisting of several steps. First, the photon energy was calibrated from the 4f spectral peak of a freshly sputtered gold wafer. Then substrate a line to set the pre-edge to be zero. Finally, the spectra were normalized to yield an edge-jump to one.

Photocatalytic activity measurement

The photocatalytic activity of all as-prepared samples were evaluated by the degradation of RhB solution under visible light irradiation. In the test, 0.01 g photocatalyst powders were dispersed into 100 mL RhB solution with the initial concentration of 15 μmol^{-1} in a quartz reactor equipped with an external cooling system, using a 300 W xenon lamp (CEL-HXF300E, CEAULIGHT Co., Ltd.) with a UV-cutoff filter ($\lambda > 400$ nm) as the visible light source. The suspension was stirred 20 min to reach the equilibrium of absorption/desorption. During the reaction, a 5 mL suspension solution

was taken at 20 min intervals, followed by centrifugation to remove the photocatalysts. In the recycling experiments, the series photocatalysts were removed and centrifuged after 3 h illumination ($\lambda > 400$ nm) for 5 times to test the stability. The degradation rates of Ag/Fe-TiO_2 sample as a function of the different wavelengths by employing a series of optical filters (365 nm, 380 nm, 420 nm, 450 nm, 475 nm, 500 nm, 550 nm, 600 nm) to isolate the broad band source into roughly monochromatic points (FWHM ~20 nm) were also investigated. The concentration of each suspension was analyzed by an UV−visible spectrophotometer (Shimadzu, UV-2600).

Computational details

All DFT calculations in the present work were performed on CASTEP code based on the plane-wave pseudopotential method. Electron exchange and correlation were approximated using the generalized-gradient approximation (GGA) with the Perdew-Burke-Ernzerhof (PBE) functional. Considering the Ag nanoparticles were mainly located on the (101) surface of TiO_2 in this work, we started from a slab model in which the Ag_4 cluster was absorbed on the (101) TiO_2 surface with a thickness of 5 layers, according to a previous report.[5] The vacuum slab perpendicular to the surface models was 12 Å, which was enough to separate the interaction between periodic images. The optimized lattice parameters of the anatase TiO_2 crystal are a = b = 3.777 Å, and c = 9.488 Å, which are in agreement with experimental value. We used a 2 × 3 × 1 Monkhorst-Pack

k-point mesh for the geometry optimization and the bottom two layers atoms were fixed as the bulk structure, while the rest of the atoms were allowed to relax freely. The cutoff energy for plane-wave was been chosen to be 380 eV. In the geometry optimization process, the energy change, maximum force, maximum stress and maximum displacement tolerance values were set to 2×10^{-5} eV per atom, 0.05 eV $Å^{-1}$, 0.1 GPa, and 0.002 Å, respectively.

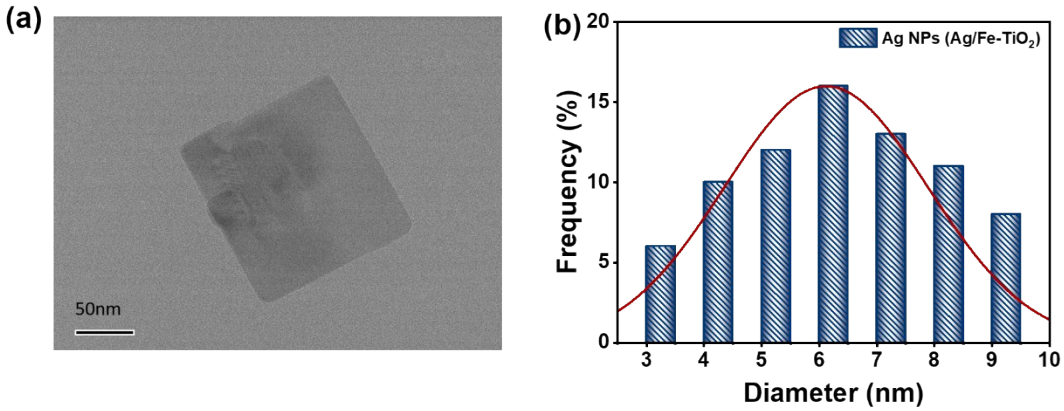

Figure S1. (a) The low magnification TEM image of TiO_2 nanoplates. (b) The size distribution of Ag NPs nanoparticles on Ag/Fe-TiO_2.

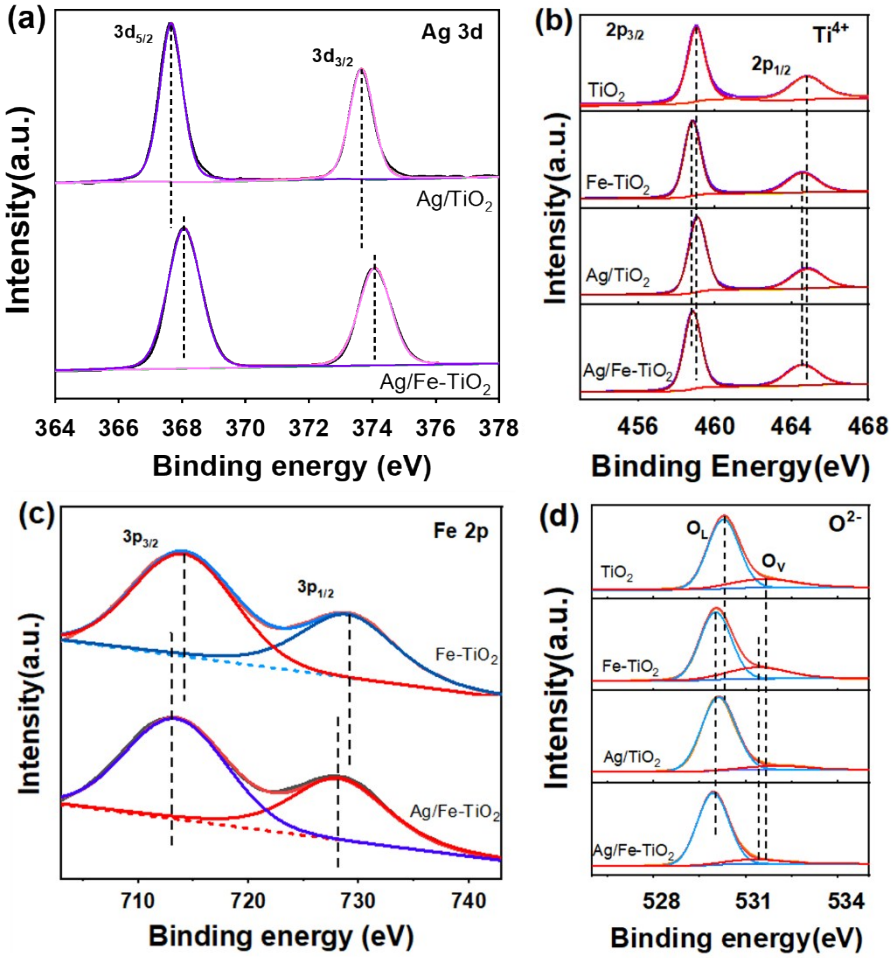

Figure S2. XPS spectra of (a) Ag 3d; (b) Ti 2p; (c) Fe 2p; (d) O 1s.

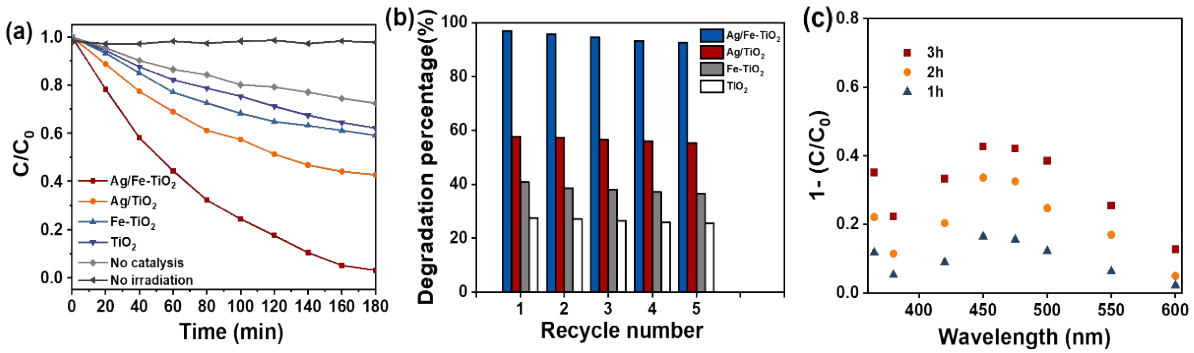

Figure S3. (a) The degradation rate of RhB solution for series sample under visible-light irradiation ($\lambda > 400$ nm). (b) Recycling test results of series sample under visible light ($\lambda > 400$ nm). (c) Degradation rate as the function of different wavelength after 1h, 2h and 3h irradiation.

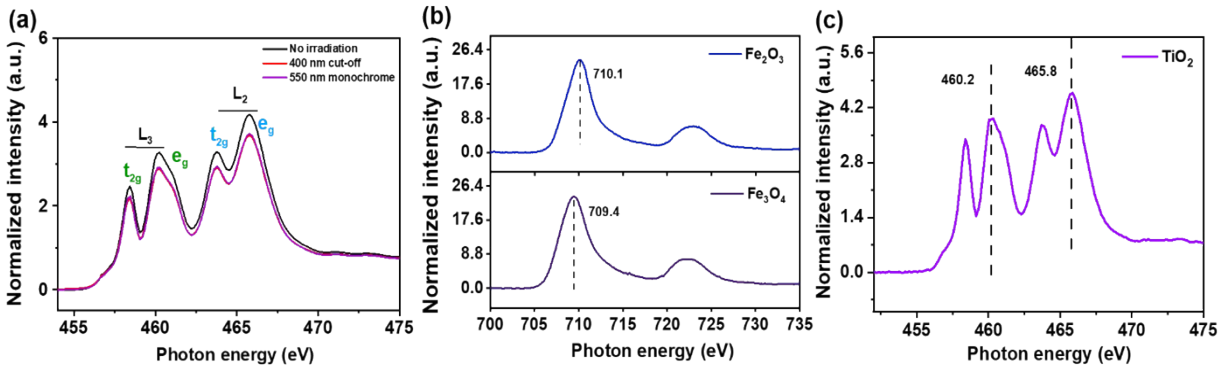

Figure S4. (a) Ti L-edge XANES of Ag/TiO_2 under different irradiation conditions. (b) Fe L-edge XANES of Fe_2O_3 and Fe_3O_4. (c) Ti L-edge XANES of pure TiO_2.

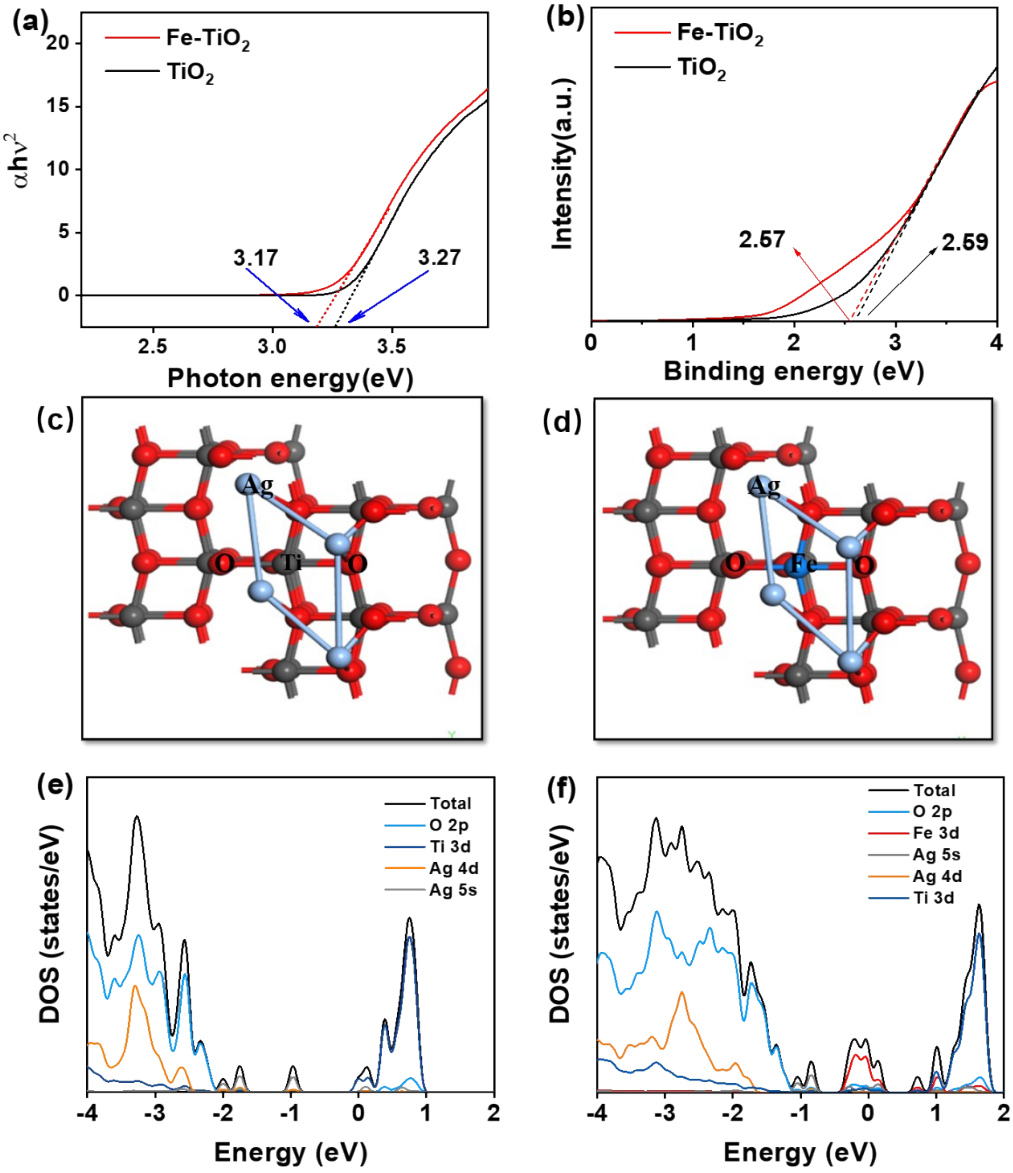

Figure S5. (a) Tauc plot for band gap determination of TiO_2 and Fe-TiO_2. (b) XPS valence band spectra of TiO_2 and Fe-TiO_2. Optimized surface structures of Ag/TiO_2 (c) and Ag/Fe-TiO_2 (d) in top view. Full and partial DOS of Ag/TiO_2 (e) and Ag/Fe-TiO_2 (f).

References

1. M. Wang, F. Zhang, X. Zhu, Z. Qi, B. Hong, J. Ding, J. Bao, S. Sun and C. Gao, *Langmuir*, 2015, **31**, 1730-1736.
2. S. Sun, J. Ding, J. Bao, C. Gao, Z. Qi, X. Yang, B. He and C. Li, *Appl. Surf. Sci.*, 2012, **258**, 5031-5037.
3. J. Xue, M. Fujitsuka and T. Majima, *ACS Appl. Mater. Interfaces.*, 2019, **11**, 40860-40867.
4. Y. Choi, H.-i. Kim, G.-h. Moon, S. Jo and W. Choi, *ACS Catal.*, 2016, **6**, 821-828.
5. P. Schlexer, A. Ruiz Puigdollers and G. Pacchioni, *Phys. Chem. Chem. Phys.*, 2015, **17**, 22342-22360.